35th Annual International Conference of the IEEE EMBS
Osaka, Japan, 3 - 7 July, 2013

Ciliary Motility Activity Measurement Using a Dense Optical Flow Algorithm

Eduardo Parrilla, Miguel Armengot, Manuel Mata, Julio Cortijo,
Jaime Riera, José L. Hueso, and David Moratal, *Senior Member, IEEE*

Abstract— **Persistent respiratory syncytial virus (RSV) infections have been associated with the exacerbation of chronic inflammatory diseases, including chronic obstructive pulmonary disease (COPD). This virus infects the respiratory epithelium, leading to chronic inflammation, and induces the release of mucins and the loss of cilia activity, two factors that determine mucus clearance and the increase in sputum volume.**

In this study, an automatic method has been established to determine the ciliary motility activity from cell cultures by means of optical flow computation, and has been applied to 136 control cultures and to 144 RSV-infected cultures.

The control group presented an average of cell surface with cilia motility per field of 41 ± 15 % (mean ± standard deviation), while the infected group presented a 11 ± 5 %, t-Student $p<0.001$. The cutoff value to classify a infected specimen was <17.89 % (sensitivity 0.94, specificity 0.93).

This methodology has proved to be a robust technique to evaluate cilia motility in cell cultures.

I. Introduction

Human respiratory syncytial virus (RSV) is an important pathogen that causes serious infection in people of all ages, including children, healthy and sick adults, and elderly individuals [1,2]. This virus results in persistent infection, leading to chronic inflammation through mechanisms involving continuous stimulation of the immune system [3,4,5]. Persistent RSV infection appears to occur in certain individuals with chronic obstructive pulmonary disease (COPD), where RSV has been associated with exacerbation of the disease, the main cause of morbidity in patients with COPD [6,7].

During COPD exacerbations, an increase occurs in sputum volume, which in the airways is the result of a balance between the ciliary beat of epithelial cells and mucin production [8]. Both processes are affected by RSV, which induces the destruction of ciliated epithelial cells and the expression of MUC5AC, the predominant mucin gene expressed in human airways [9,10,11,12].

The main objective of this study was to establish an automatic method to evaluate the cilia motility of cultures and its sensitivity to differentiate a control culture versus a culture with cells infected with RSV.

II. Materials and Methods

A. Cell model, control, and experimental group

Human lung tissue was obtained from patients who had undergone surgery for lung carcinoma, as previously outlined [13].

Experiments were approved by the local ethics committee and informed consent was obtained. None of the patients were being chronically treated.

Bronchia were carefully dissected free from adjoining connective tissue and lung parenchyma. Human bronchial epithelial cells were cultured and differentiated. In brief, a multilayered bronchial epithelium was obtained by seeding cells (8.25×10^4 cell per insert) onto polyester inserts (Millipore, Billerica, MA). Cells were submerged in differentiation medium for the first 7 days.

Cells were then cultured for an additional 21 days with the apical surface exposed to air, and ciliary activity was inspected every day until the maximal density of ciliated cells (200–250 ciliated cells per field) was reached. Cultures were then washed three times with fresh differentiation culture medium and infected with 100 mL of the same media containing 2×10^6 plaque forming units RSV per insert. Cultures were incubated for 2 h at 37 ºC and washed once with 500 µL differentiation media.

Infected cultures were maintained until day 15 postinfection. Culture medium was replaced every 48 h.

In this study, two different groups were considered: control (mock-infected cells), and infected (cells infected with RSV).

B. Image acquisition

Ciliary cells cultures were mounted onto the stage of a Nikon Eclipse TE100 microscope, by using a 40x Nikon lens with a final optical gain of 400x. The microscope was connected to a CCD camera (Digital Quad High Speed Progressive Scan Camera, JAI CV-A33 CL) that records images with a matrix size of 649×494 pixels, and a rate of

The support of the Spanish Ministry of Economy and Competitiveness through project TEC2012-33778 and of the *Vicerectorado de Investigación* of the Universitat Politècnica de València through project "*Proyectos de Nuevas Líneas de Investigación Multidisciplinares*" PAID-05-10/2697 is acknowledged.

E. Parrilla is with the Biomechanics Institute of Valencia, Valencia, Spain

M. Armengot is with the Primary Ciliary Dysquinesia Unit of the General and University Hospital, Valencia University, Valencia, Spain

M. Mata and J. Cortijo are with the Researh Department, General and University Hospital, Valencia University, Valencia, Spain

J. Riera and J. L. Hueso are with the Institute of Multidisciplinary Mathematics, Universitat Politècnica de València, Valencia, Spain

D. Moratal is with the Center for Biomaterials and Tissue Engineering, Universitat Politècnica de València, Valencia, Spain (corresponding author e-mail: dmoratal@eln.upv.es).

120 frames per second. Images were acquired into a HP Workstation xw6200 Xeon 3.4 GHz with 2Gb of RAM system by means of an image acquisition board (NI PCIe-1429, Full Configuration Camera Link Image Acquisition).

C. Ciliary motility activity measurement

For computing the ciliary motion, it is necessary to calculate the movement of the pixels between each frame and the initial frame. This motion has been computed by using the Farnebäck method [14], which uses polynomial expansion to approximate the neighbors of a pixel. This dense optical flow analysis produces a displacement field from two video frames.

The idea behind polynomial expansion is to approximate the image intensity in a neighborhood of each pixel with a set of polynomial functions. We are only interested in quadratic polynomials, giving us the local signal model, expressed in a local coordinate system,

$$f(\mathbf{x}) \approx \mathbf{x}^{\mathbf{T}}\mathbf{A}\mathbf{x} + \mathbf{b}^{\mathbf{T}}\mathbf{x} + c \tag{1}$$

where $\mathbf{A}$ is a symmetric matrix, $\mathbf{b}$ a vector and c a scalar. The coefficients are estimated from a weighted least squares fit to the signal values in the neighborhood.

Following the description in Farnebäck and Westin [15], to derive the expression for the translation, we first consider a polynomial expansion of the signal, f_1, and a version of the signal that has been globally translated, f_2, by the vector $\mathbf{d}$.

$$f_1(\mathbf{x}) = \mathbf{x}^T\mathbf{A}_1\mathbf{x} + \mathbf{b}_1^T\mathbf{x} + c_1 \tag{2}$$

$$\begin{aligned} f_2(\mathbf{x}) &= f_1(\mathbf{x}-\mathbf{d}) = (\mathbf{x}-\mathbf{d})^T\mathbf{A}_1(\mathbf{x}-\mathbf{d}) + \mathbf{b}_1^T(\mathbf{x}-\mathbf{d}) + c_1 \\ &= \mathbf{x}^T\mathbf{A}_1\mathbf{x} + (\mathbf{b}_1 - 2\mathbf{A}_1\mathbf{d})^T\mathbf{x} + \mathbf{d}^T\mathbf{A}_1\mathbf{d} - \mathbf{b}_1^T\mathbf{d} + c_1 \\ &= \mathbf{x}^T\mathbf{A}_2\mathbf{x} + \mathbf{b}_2^T\mathbf{x} + c_2 \end{aligned} \tag{3}$$

Equating the coefficients in the quadratic polynomials yields

$$\mathbf{A}_2 = \mathbf{A}_1 \tag{4}$$

$$\mathbf{b}_2 = \mathbf{b}_1 - 2\mathbf{A}_1\mathbf{d} \tag{5}$$

$$c_2 = \mathbf{d}^T\mathbf{A}_1\mathbf{d} - \mathbf{b}_1^T\mathbf{d} + c_1 \tag{6}$$

The key observation is that by equation (5) we can solve for the translation $\mathbf{d}$, at least if $\mathbf{A}_1$ is non-singular,

$$\mathbf{d} = -\frac{1}{2}\mathbf{A}_1^{-1}(\mathbf{b}_2 - \mathbf{b}_1) \tag{7}$$

We note that this observation holds for any signal dimensionality.

For motion analysis, we start by doing a polynomial expansion of both the left and the right images, giving us expansion coefficients $\mathbf{A}_l(x, y)$, $\mathbf{b}_l(x, y)$, and $c_l(x, y)$ for the left image and $\mathbf{A}_r(x, y)$, $\mathbf{b}_r(x, y)$, and $c_r(x, y)$ for the right image.

The first practical complication is that equation (4) assumes that the $\mathbf{A}$ matrix should be the same in both images.

As a practical solution, the arithmetic mean can be used,

$$\mathbf{A}(x, y) = \frac{\mathbf{A}_l(x, y) + \mathbf{A}_r(x, y)}{2} \tag{8}$$

There are less difficulties with $\mathbf{b}$ and we can directly use $\mathbf{b}_r$ as $\mathbf{b}_1$ and $\mathbf{b}_l$ as $\mathbf{b}_2$. To simplify later steps of the algorithm we introduce

$$\Delta\mathbf{b}(x, y) = -\frac{1}{2}(\mathbf{b}_l(x, y) - \mathbf{b}_r(x, y)) \tag{9}$$

This turns equations (5) and (7) into

$$\mathbf{A}(x, y)\mathbf{d}(x, y) = \Delta\mathbf{b}(x, y) \tag{10}$$

$$\mathbf{d}(x, y) = \mathbf{A}(x, y)^{-1}\Delta\mathbf{b}(x, y) \tag{11}$$

In principle, we should now be able to obtain a displacement vector at (x, y) from equation (11).

In order to compute the movement percentage of each video sequence, two criterions to decide if a pixel has moved must be established. Firstly, it is necessary to know, for each frame of the image sequence, how many pixels have motion with respect to the initial frame. To perform this task, the optical flow between the two frames must be computed and it will be considered that a pixel has moved if the magnitude of its displacement is greater than a certain threshold. This frame-to-frame threshold th_f will depend on the size of the cells in the image. Secondly, it is necessary to define a minimum number of frames where a certain pixel presents motion, in order to consider that the pixel has moved throughout the sequence. In this way, a final threshold th_t that will be a percentage of the total frames in the sequence has been applied. Finally, we calculate the movement percentage of the video as the percentage of pixels that have motion regarding the total number of pixels in the image.

D. Statistical analysis

The exposed technique has been applied to 280 phase-contrast microscopy image sequences corresponding to 2 different subjects. The average length of the video sequences is 1156 ± 118 frames (mean ± standard deviation), from which 136 sequences correspond to control cultures and 144 to infected cultures. Analysis of the cultures was done at days 0, 8, 10, and 15 post-infection. The sequences corresponding to day 0 were excluded from the group comparison, and thus only 205 image sequences were considered for the group comparison: 99

corresponding to the control group and 106 to the infected group.

For the ciliary motility activity measurement, a threshold th_f = 0.3 has been selected empirically to optimize the detection of the movement, and the value of the threshold th_t has been chosen as the half of the total number of frames for each video.

Statistical analyses were performed with SPSS for Windows, version 16 (IBM, Somers, NY, USA). Student-t test was used to compare the two groups. Values of continuous variables were expressed as mean ± standard deviation. Receiver operating characteristics (ROC) analysis was applied to evaluate the average of cell surface with cilia motility per field as a diagnostic tool. The performance of the classifiers was evaluated by the area (Az) and confidence interval at 95% (CI95%) under the ROC curve.

III. Results

Fig. 1 shows an example of a human bronchial epithelial cell image together with its ciliary motility activity measurement.

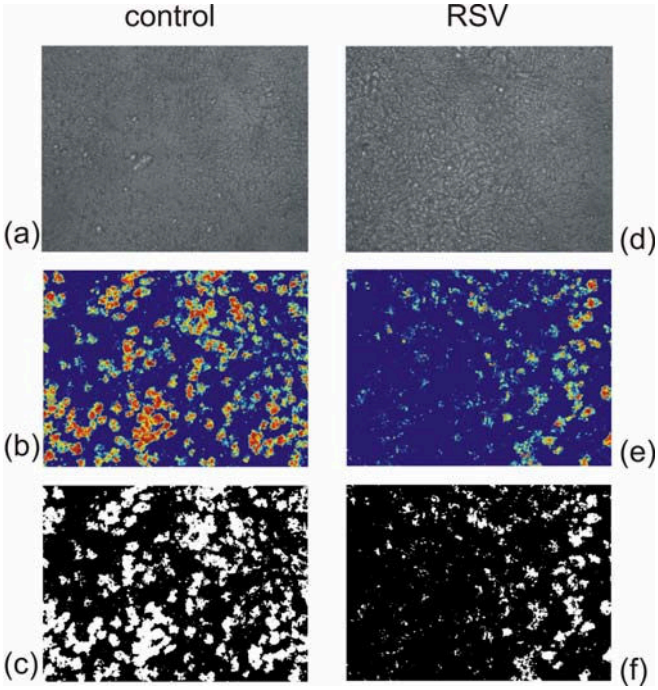

Figure 1. Human bronchial epithelial cell images corresponding to a control (a-c) and to an RSV-infected culture (d-f). (a, d) Phase-contrast microscopy image. (b,e) Ciliary motility activity measurement obtained over the original images. (c,f) Binarized image of (b,e) showing the quantity of ciliary motility.

Fig. 2 shows the time effect on the cilia motility of the cultured cells for the 15 days post-infection.

The average of cell surface with cilia motility per field as a diagnostic tool provided an Az 0.97 (CI95%, 0.95-0.99). The cutoff value to classify a infected specimen was <17.89 % (sensitivity 0.94, specificity 0.93). Fig. 3 depicts a distribution of the average motility from the eighth day on.

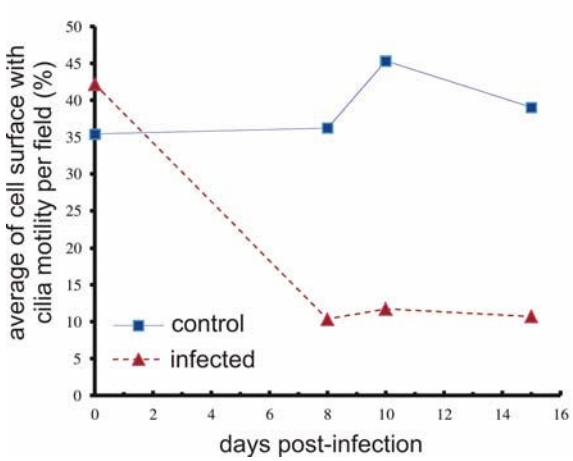

Figure 2. Time effect (days 0, 8, 10 and 15) on the cilia motility of the cells.

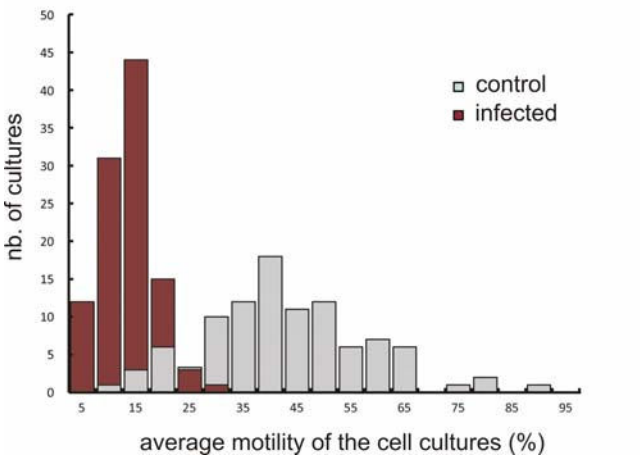

Figure 3. Distribution of the average motility of the cells in control and infected cultures from the eighth day on.

Concerning the dependence of the calculated motility on the selection of the threshold values of th_f and th_t, there is a dependence of the movement percentage on these threshold values although the ratio of percentages between different videos remains practically constant, and thus the results of this study also does.

IV. Conclusion

An automatic method to determine cilia motility in phase-contrast microscopy images of cell cultures has been presented.

The ciliary motility activity has been usually performed manually by experts, counting under double-blind conditions to minimize experimental errors due to the observer. This is a huge time-consuming task, and it is always subjected to experimental errors. The methodology presented in this study has proved to be robust, providing an extremely high index of diagnostic performance.

REFERENCES

[1] P. L. Collins, R. M. Chanock, B. R. Murphy, "Respiratory syncytial virus". In: Knipe D, et al., editors. Virology, 4th ed., New York: Raven Press, 2001, pp. 1443–1485.

[2] I. Martínez, L. Lombardía, B. García-Barreno, O. Domínguez, J. A. Melero, "Distinct gene subsets are induced at different time points after human respiratory syncytial virus infection of A549 cells," *Gen Virol*, vol. 88, pp. 570–581, 2007

[3] S. Krishnan, M. Halonen, R. C. Welliver, "Innate immune responses in respiratory syncytial virus infections," *Viral Immunol*, vol. 17, pp. 220–33, 2004

[4] I. Martínez, L. Lombardía, C. Herranza, B. García-Barreno, O. Domínguez, J. A. Melero, "Cultures of HEp-2 cells persistently infected by human respiratory syncytial virus differ in chemokine expression and resistance to apoptosis as compared to lytic infections of the same cell type," *Virology*, vol. 388, pp. 31–41, 2009.

[5] F. Di Rosa, V. Barnaba, "Persisting viruses and chronic inflammation: understanding their relation to autoimmunity," *Immunol Rev*, vol. 164, pp. 17–27, 1998.

[6] T. M. Wilkinson, G. C. Donaldson, S. L. Johnston, P. J. Openshaw, J. A. Wedzicha, "Respiratory syncytial virus, airway inflammation, and FEV1 decline in patients with chronic obstructive pulmonary disease," *Am J Respir Crit Care Med*, vol. 173, pp.871–876, 2006.

[7] J. A. Wedzycha, "Role of viruses in exacerbations of chronic obstructive pulmonary disease," *Proc Am Thorac Soc*, vol. 1, pp. 115–120, 2004.

[8] P. Malia, S. L. Johnson, "How viral infections causes exacerbations of airway diseases," *Chest*, vol. 130, pp. 1203–10, 2006.

[9] D. A. Tristram, W. Hicks Jr, R. Hard, "Respiratory syncytial virus and human bronchial epithelium," *Arch Otolaryngol Head Neck Surg*, vol. 124, pp. 777–783, 1998.

[10] V. Avadhanula, C. A. Rodriguez, J. P. Devincenzo, Y. Wang, R. J. Webby, G. C. Ulett, E. E. Adderson, "Respiratory viruses augment the adhesion of bacterial pathogens to respiratory epithelium in a viral species- and cell type-dependent manner," *J Virol*, vol. 80, pp. 1629–1636, 2006.

[11] M. Fishaut, J. D. Schwartzman, K. McIntosh, S. R. Mostow, "Behavior of respiratory syncytial virus in piglet tracheal organ culture," *J Infect Dis*, vol. 138, pp. 644–649, 1978.

[12] K. Takeyama, J. V. Fahy, J. A. Nadel, "Relationship of epidermal growth factor receptors to goblet cell production in human bronchi," *Am J Respir Crit Care Med*, vol. 163, pp. 511–516, 2001.

[13] M. Mata, B. Sarriá, A. Buenestado, J. Cortijo, M. Cerda, E. J. Morcillo, "Phosphodiesterase 4 inhibition decreases MUC5AC expression induced by epidermal growth factor in human epithelial cells," *Thorax*, vol. 60, pp. 144–152, 2005.

[14] G. Farnebäck, "Two-Frame Motion Estimation Based on Polynomial Expansion, " *SCIA, Lecture Notes in Computer Science*, vol. 2749, pp. 363-370, Springer, 2003.

[15] G. Farnebäck, C.-F. Westin, "Affine and deformable registration based on polynomial expansion," in *Ninth International Conference on Medical Image Computing and Computer-Assisted Intervention (MICCAI'06), Lecture Notes in Computer Science*, vol. 4191, pp. 857-864, Copenhagen, Denmark, 2006.